Cancer Letters 459 (2019) 216–226

Contents lists available at ScienceDirect

Cancer Letters

journal homepage: www.elsevier.com/locate/canlet

Original Articles

The circular RNA circ-Ccnb1 dissociates Ccnb1/Cdk1 complex suppressing cell invasion and tumorigenesis

Ling Fang[a,b], William W. Du[a], Faryal Mehwish Awan[a,c], Jun Dong[a,d,**], Burton B. Yang[a,e,*]

[a] Sunnybrook Research Institute, Toronto, Canada
[b] China-Japan Union Hospital of Jilin University, Jilin, China
[c] Atta-ur-Rahman School of Applied Biosciences (ASAB), National University of Sciences and Technology (NUST), H-12, Islamabad, Pakistan
[d] The Second Affiliated Hospital of Guangzhou Medical University, Guangzhou, China
[e] Department of Laboratory Medicine and Pathobiology, University of Toronto, Toronto, Canada

ARTICLE INFO

Keywords:
Circular RNA
circ-Ccnb1
Ccnb1
Cdk1
Tumorigenesis

ABSTRACT

Circular RNAs represent a large class of non-coding RNAs that are extensively expressed in mammals. However, the functions of circular RNAs are largely unknown. We recently reported that the circular RNA circ-Ccnb1 could bind with H2AX in p53 mutant cells and suppressed mutant p53 in tumor progression. Here we found that circ-Ccnb1 could interact with both Ccnb1 and Cdk1 proteins. Normally, Ccnb1 and Cdk1 proteins form a complex, allowing Ccnb1 to function as an all-or-none switch for cell mitosis. The interaction of circ-Ccnb1 with Ccnb1 and Cdk1 proteins dissociated the formation of Ccnb1-Cdk1 complex, by forming a large complex containing circ-Ccnb1, Ccnb1 and Cdk1. Formation of this large complex may occur in cytosol and nuclei, and Ccnb1 loses its roles in enhancing cell migration, invasion, proliferation and survival. In vivo, ectopic delivery of circ-Ccnb1 inhibited tumor growth and extended mouse viability. These results have added another layer of mechanisms for circ-Ccnb1 to regulate tumor progression in vitro and in vivo.

1. Introduction

Circular RNAs are a large class of single-stranded RNAs grouped as non-coding RNAs with a widespread expression pattern [1–3]. Genome-wide analyses of RNA sequencing data from mouse and human cells have revealed evolutionary conservation of the circular RNAs, suggesting specific roles of circular RNAs in cellular physiology [4–6]. Most circular RNAs appear to be generated from exons, known as exonic circular RNAs [3,5]. There is a large group of circular RNAs that are generated from introns, called intronic circular RNAs [7]. In addition, some circular RNAs contain exons and introns, called ciRNAs, producing exon-intron circRNAs or EIciRNAs [8]. It is reported that exonic circular RNAs are mainly detected in the cytoplasm, while intronic circular RNAs are predominately found in the nuclei [4]. If the exonic circular RNAs are highly expressed in the cytoplasm and contain multiple microRNA binding sites, they may function as microRNA sponges to arrest microRNA activities [9–11]. Due to their increased stability, circular RNAs may be more effective than linear transcripts [2,12]. Some circular RNAs can interact with proteins which form RNA-protein complex and regulate their activity [13,14]. We have found that circular RNAs not only bind proteins but also regulate nuclear translocation of the proteins and increase cell proliferation [15–17]. Many circular RNAs have been known to play roles in cancer development [18–20].

Cyclin B1 (Ccnb1) is a regulatory protein involved in cell proliferation. Ccnb1 binds to Cyclin-dependent kinase 1 (Cdk1) to form a complex. The complex phosphorylates target substrates and leads to cell cycle progression. As the key regulatory molecule in cell cycle progression, Cdk1 is a highly conserved and highly regulated protein that acts as a serine/threonine kinase. The binding with Ccnb1 alters the access to the active site of Cdk1 and contributes to the switch-like event determining whether mitosis will start. Once the Ccnb1-Cdk1 complex is activated, it can no longer be deactivated. The activated Ccnb1-Cdk1 complex will initiate several steps in mitosis including condensation of chromosomes, assembly of spindle pole and breakdown of nuclear envelope. Increased expression of Ccnb1 has been detected in a number of cancers [21,22]. High levels of Ccnb1 are associated with immortalization of the tumor cells and chromosomal instability that

Abbreviations: DMEM, Dulbecco's modified Eagle's medium; FBS, fetal bovine serum; GFP, green fluorescent protein

* Corresponding author. S-Wing Research Building, 2075 Bayview Ave, Toronto M4N 3M5, Canada.
** Corresponding author. The Second Affiliated Hospital of Guangzhou Medical University, Guangzhou, China.
E-mail addresses: dongjunrain@sina.com (J. Dong), byang@sri.utoronto.ca (B.B. Yang).

https://doi.org/10.1016/j.canlet.2019.05.036
Received 8 April 2019; Received in revised form 22 May 2019; Accepted 24 May 2019

contributes to tumor cell invasion and prognosis of cancer patients [23]. In particular, Ccnb1 is significantly higher in breast cancer tissue and strongly associated with lymph node metastasis [24]. Increased nuclear levels of Ccnb1 lead to poorer prognosis [25]. This is not only observed in breast cancer but also in head and neck squamous cell cancer and esophageal cancer [26]. Our current study shows that a circular RNA circ-Ccnb1 can inhibit the formation of the Ccnb1-Cdk1 complex and modulate nuclear translocation of these two molecules, thus inhibiting tumor progression.

2. Materials and methods

2.1. Constructs

A construct expressing human circular RNA Ccnb1 (circ-Ccnb1) was generated by us. The plasmids contained a Bluescript backbone, a CMV promoter driving mouse circ-Ccnb1 or a non-related sequence serving as a control. The green fluorescent protein (GFP) expression unit was driven by another CMV promoter separately.

2.2. Nuclear extract preparation

Cell cultures were lysed using 1 ml nuclear extraction buffer (20 mM Hepes, pH 7.2, 10 mM KCl, 2 mM MgCl2 and protease inhibitors). The cells were homogenized with a prechilled Dounce homogenizer with 20 strokes. The lysis was subject to centrifugation at 4200 rpm for 5 min. The pellet was washed 3 times with PBS and resuspended in 100 μl lysis buffer containing 0.5 M NaCl. After centrifugation at 13,200 rpm for 10 min, supernatants containing nuclear extract were obtained for further analysis.

2.3. Western blot

Cells were lysed and subject to sodium dodecyl sulfate-polyacrylamide gel electrophoresis (SDS-PAGE) containing 10% acrylamide gel, which was subjected to electrophoresis at 80 voltages at 4 °C for 3 h. The separated proteins were transferred onto a nitrocellulose membrane using semi-dry approach. The membrane was blocked in a buffer containing 10 mM Tris-Cl, pH 8.0, 150 mM NaCl, 0.05% Tween-20, and 5% non-fat dry milk powder for 0.5 h, and then incubated with primary antibodies at 4 °C overnight. The primary antibodies against Ccnb1 and Cdk1 were from Cell Signaling (Danvers, MA, USA). The membrane was washed with the same buffer without milk for three times, 30 min each. The washed membrane was incubated with secondary antibodies for 2 h. After washing, the bound antibodies were visualized with an ECL detection kit.

2.4. RT-PCR and real-time PCR

Cell cultures (2×10^6 cells) were harvested to isolate total RNA using the Qiagen RNeasy mini kit. Two micrograms of total RNA were used to synthesize cDNA, a portion of which (1 μl, equal to 0.2 μg cDNA) was used in a PCR with appropriate primers. Real-time PCR were performed with miScriptSYBR GreenPCR Kit (Qiagen) using 1 μl cDNA as template. The primers used for circ-Ccnb1 were 5′ tgatcggttcatgcaggttgatac and 5′ tccagatgtttccattgggcttgg. The primers used for Ccnb1 mRNA were 5′ ggtacctatgctggtgccagtgcc and 5′ catcagagaaagcctgacacaggt.

2.5. Immunoprecipitation assays

In protein-protein precipitation assay, a total of 10^7 cells were washed with ice-cold phosphate-buffered saline, and lysed in 1 ml lysis buffer. Equal amounts of protein were incubated with 5 μg primary antibody and 50 μl of 50% slurry of protein A-Sepharose at 4 °C for 4 h. The pellet was washed 3 times with PBS and were resuspended in 2 × Laemmli buffer (0.125 M Tris-HCl, 4% SDS, 20% glycerol, 10% 2-mercaptoethanol, 0.004% bromphenol blue, pH6.8), and subject to Western blotting probed with antibodies against the other proteins.

In RNA precipitation assay, 10^7 cells were washed in ice-cold PBS, lysed in 500 μl co-IP buffer, (50 mM HEPES, pH 7.5, 150 mM NaCl, 1 mM EDTA, 5 mM EGTA, 1% (w/v) Tween 20, 1 mM dithiothreitol, 1 mM NaF, 100 μM PMSF), and incubated with 5 μg primary antibodies at 4 °C for 2 h. 40 μl of 50% slurry of protein A-Sepharose was added to each sample. The mixtures were incubated at 4 °C for 4 h and then subject to brief centrifugation. The pellets were washed with PBS for three times and resuspended in 0.5 ml Tri Reagent (Sigma-Aldrich). The elutes were subject to reverse transcription and PCR to detect the presence of the binding RNA using respective primers.

In RNA pull-down assay, 10^7 cells were washed in ice-cold phosphate-buffered saline, lysed in 500 μl co-IP buffer, and incubated with 3 μg biotinylated DNA probes of circ-Ccnb1 (probe sequence: 5' gagaggcagtatcaacctgcatgaaccgatca) at room temperature for 2 h. 50 μl washed Streptavidin C1 magnetic beads (Invitrogen) were added to each binding reaction and further incubated at room temperature for another 1 h. Beads were washed briefly with co-IP buffer for 5 times. RNAs in the pull-down materials were determined with RT-PCR. The bound proteins in the pull-down material were analyzed by Western blotting probed with antibodies against the RNA-binding proteins.

2.6. Tumor formation assay

Tumorigenesis was performed as described previously [27,28]. All animal experiments were conducted according to the guidelines approved by the Animal Care Committee at Sunnybrook Research Institute (Protocol Number, AUP 15–076). Animals were kept in the Animal Core Facility of Sunnybrook Research Institute for one week before use. Two survival assays were performed.

In one of the survival assays, four-week old C57BL mice were randomly divided into 2 groups: a control group and circ-Ccnb1 group. Each group had 20 mice. All mice were injected intraperitoneally with B-16 cells (B16F10, 2×10^4 cells/mouse). Mouse viability was monitored for up to 35 days.

In the other assay, four-week old C57BL mice were randomly divided into 4 groups: oligo control, blocking oligo for Cdk1-binding site, blocking oligo for Ccnb1-binding site, and blocking for both binding sites. Each group had 20 mice. All mice were injected intraperitoneally with B-16 cells (2×10^4 cells/mouse). Next day after cell injection, these oligos were conjugated with PEG-Au NP complexes and injected intraperitoneally at a dose of 5 μg/mouse. Formulation of the complexes (oligo-PEG-AuNP) was performed as previously described [29]. Briefly, 750 μg oligo was dissolved in 800 μl RNase-free water. The mPEGSH (PG1-TH-2k, Nanocs) was mixed with the oligos (1:20 M ratio). Then 10-nm gold nanoparticles (AuNP, Cytodiagnostics) were mixed with the oligos at a weight ratio of 1:20. The mixture was gently shaken at 60 °C for 30 min. The mixture was then transferred into a syringe, followed by the injection into mice intraperitoneally. This was repeated every three days until the experiment was completed in 43 days. Mouse viability was monitored.

2.7. Identification of binding sites

To determine the interaction between circ-Ccnb1 with Cdk1 and Ccnb1, we used the protein-RNA docking analysis tool NPDock Server [30] that generated 20,000 models to identify the best binding one. NPDock Server combined GRAMM for docking, scoring, clustering followed by refinement of best scored docked complex. Residue-level resolution contact maps of circ-Ccnb1-Cdk1 and circ-Ccnb1-Ccnb1 docked complexes were determined using RNAmap2D as described [31]. The contact distances between Cα atoms of protein residues and O5′ atoms of RNA strands were determined. Two residues were considered in contact when their O5′–Cα distance is less than 10 Å.

Distance-based approach was used to identify the binding site for the protein-RNA complex. Two atoms (one in RNA and the other in protein) were considered binding to each other if the distance between them was < 3.5 Å.

2.8. Statistical analysis

All experiments were performed in triplicate and numerical data were subject to independent sample *t*-test. The levels of significance were set at $*p < 0.05$ and $**p < 0.01$. Error bars represent SD (n = 4 if no indicated).

3. Results

3.1. Circ-ccnb1 interaction with Ccnb1 and Cdk1

Our previous study showed that expression of circ-Ccnb1 inhibited cell growth [32]. We hypothesized that circ-Ccnb1 interacted with some cell cycle-associated proteins and exerted its role in cell proliferation. To test this, we prepared cell lysate from HTB-126 cells and incubated the lysate with antibodies against cell cycle proteins including cyclin A (Ccna), Ccnb1, Ccnd1, Ccne, Cdk1, Cdk2, Cdk4, Cdk6, p16, p18, p21, and p27. Antibodies against rabbit IgG and mouse IgG were used as controls. The precipitated products were subjected to real-time PCR with primers amplifying circ-Ccnb1 and Ccnb1 mRNA. We found that the anti-Ccnb1 and anti-Cdk1 antibodies precipitated significantly higher levels of circ-Ccnb1 but not the linear Ccnb1 mRNA (Fig. 1A). Some other antibodies appeared to be able to precipitate circ-Ccnb1, but the precipitated amounts were much lower than antibodies against Ccnb1 and Cdk1. In HTB-126 cells transfected with circ-Ccnb1 or the vector, the antibodies precipitated significantly higher levels of circ-Ccnb1 in the circ-Ccnb1 transfected cells relative to control (Fig. 1B). The lysates prepared from HTB-126 cells transfected with circ-Ccnb1 or the vector were incubated with the probe specifically recognizing circ-Ccnb1 or a control oligo, followed by Western blotting. The circ-Ccnb1 probe could only pull down Ccnb1 and Cdk1 (Fig. 1C). To test whether endogenous circ-Ccnb1 was involved in binding to Ccnb1 and Cdk1, we transfected MDA-MB231 cells with siRNA targeting circ-Ccnb1 (target sequence: 5' cgguucaugcagguugaua), followed by pull down assays. It was confirmed that silencing circ-Ccnb1 significantly decreased the antibodies against Ccnb1 and Cdk1 precipitating circ-Ccnb1 (Fig. 1D). In the siRNA-transfected cells, the circ-Ccnb1 probe pulled down decreased levels of Ccnb1 and Cdk1 (Fig. 1E).

We analyzed the potential interaction of circ-Ccnb1 with Ccnb1 and Cdk1 using a computer algorithm as performed previously [33]. The predicted secondary structure of circ-Ccnb1 was analyzed using the formula $\Delta G = \Delta H - T\Delta S$, $\Delta G = -69.60$ kcal/mol at 37 °C, $\Delta H = -886.90$ kcal/mol, and $\Delta S = -2635.1$ cal/(K·mol). T(K) is the absolute temperature and ΔH, ΔG, ΔS, denote the change in enthalpy, free energy, and entropy, respectively. The secondary structure was analyzed by the RNA composer software for tertiary prediction. The molecular simulation predicted a minimal binding region of circ-Ccnb1 for Ccnb1 and Cdk1, and the essential nucleotides in binding to Ccnb1 and Cdk1 are marked (Fig 1F). In the absence of circ-Ccnb1, Ccnb1 and Cdk1 formed a compact complex (Fig 1G). The essential nucleotides in binding to Ccnb1 and Cdk1 are marked (Fig. 1F). In the presence of circ-Ccnb1, the circular RNA interacted with both Ccnb1 and Cdk1 to form a complex (Fig. 1H). The individual interaction between circ-Ccnb1 with Ccnb1 and Cdk1 are shown in Fig. 1I.

To test whether circ-Ccnb1 played roles in mediating Ccnb1 and Cdk1 interaction, we performed a co-immunoprecipitation assay. Cell lysates were prepared from circ-Ccnb1-and vector-transfected HTB126 cells and subject to Western blotting with anti-Ccnb1 and anti-Cdk1 antibodies. It showed that anti-Ccnb1 antibody detected similar levels of Cdk1 and Ccnb1 in the circ-Ccnb1-transfected cells (Fig. 2A). Silencing endogenous circ-Ccnb1 did not affect expression of Ccnb1 and Cdk1 (Fig. 2B). To confirm that the bridging effect of circ-Ccnb1 on Ccnb1 and Cdk1 interaction did not occur through other factors but relied on circ-Ccnb1 circular RNA, we treated the cell lysates with RNase A that degraded the circular RNA. The experiment confirmed that in the presence of RNase A, anti-Ccnb1 antibody could no longer precipitate Cdk1 in the cells transfected with circ-Ccnb1 and vice versa (Fig. 2C).

Finally, we designed blocking oligos for Ccnb1 and Cdk1 binding sites. HTB126 cells were transfected with circ-Ccnb1, vector, bl-Ccn (blocking oligo for Ccnb1 binding site), bl-Cdk (blocking oligo for Cdk1 binding site), and both (both blocking oligos). Cell lysates were prepared and incubated with circ-Ccnb1 probe to pull down the circular RNA and its potential binding proteins. Western blot analysis revealed that transfection with the bl-Ccn decreased Ccnb1 precipitation, while transfection with bl-Cdk inhibited circ-Ccnb1 pulling down Cdk1 (Fig. 2D).

3.2. Circ-ccnb1 modulates nuclear translocation of Ccnb1 and Cdk1

It has been reported that exonic circular RNAs are mainly expressed in the cytosol [4]. However, Ccnb1 and Cdk1 functions in nuclei [34]. We thus determined localization of circ-Ccnb1 by preparing the cytoplasmic and nuclear fractions of HTB126 cells. Real-time PCR analysis revealed that circ-Ccnb1 was mainly detected in the nuclei (Fig. 3A). In the circ-Ccnb1-transfected cells, the circ-Ccnb1 probe pulled down significantly higher levels of circ-Ccnb1 than the control oligo (Fig. 3B). On Western blotting, we found that ectopic expression of circ-Ccnb1 decreased nuclear translocation of Ccnb1 and Cdk1 proteins (Fig. 3C). After cross-linking treatment, we confirmed that antibodies against Ccnb1 and Cdk1 could precipitate circ-Ccnb1 but not linear Ccnb1 mRNA in the nuclei (Fig. 3D). Ectopic expression significantly increased antibodies against Ccnb1 and Cdk1 pulling down circ-Ccnb1 (Fig. 3E). On the other hand, silencing circ-Ccnb1 inhibited circ-Ccnb1 probe pulling down circ-Ccnb1 in the nuclei (Fig. 3F) but increased nuclear translocation of Ccnb1 and Cdk1 (Fig. 3G).

To examine the nuclear translocation of Ccnb1 and Cdk1, we prepared nuclear fractions from HTB126 cells transfected with circ-Ccnb1 and the vector, followed by pull down assay. The circ-Ccnb1 probe pulled down much more Cdk1 and Ccnb1 (Fig. 4A). Silencing endogenous circ-Ccnb1 decreased anti-Cdk1 antibody precipitating Ccnb1 and vice versa (Fig. 4B). The blocking oligos were then transfected into HTB126 cells. After confirming equal expression of Ccnb1 and Cdk1 in the cells, the lysates were incubated with circ-Ccnb1 probe or the control oligo. It showed that transfection with either oligo that blocked Ccnb1 binding site or Cdk1 binding site did not affect nuclear translocation of Ccnb1 and Cdk1. However, transfection with both blocking oligos increased nuclear translocation of Ccnb1 and Cdk1 (Fig. 4C). This confirmed that the complex contained circ-Ccnb1, Ccnb1 and Cdk1.

HTB126 cells were then transfected with vector, circ-Ccnb1, circ-Ccnb1 (without cross-liking), bl-Cdk, bl-Ccn, and both, followed by cross-linking. Lysates were prepared and incubated with the circ-Ccnb1 probe to pull down Ccnb1 and Cdk1. It showed that transfection with the blocking oligos decreased pull down levels of the related proteins (Fig. 4D). Un-crosslinking could also decrease circ-Ccnb1 pulling down Ccnb1 and Cdk1. Based on these results, a diagram showing the effect of circ-Ccnb1 on mediating the interaction of Ccnb1 and Cdk1 was reached (Fig. 4E).

3.3. The in vitro effects of circ-Ccnb1 interaction with Ccnb1 and Cdk1

We examined the effect of circ-Ccnb1 binding with Ccnb1 and Cdk1 on regulating cell activities. In cell migration assays, we found that overexpression of circ-Ccnb1 significantly inhibited migration in HTB126 (Fig. 5A) and B16 cells (Fig. 5B). Silencing circ-Ccnb1 in MDA-MB-231 cells increased cell migration (Fig. 5C). To test effects of

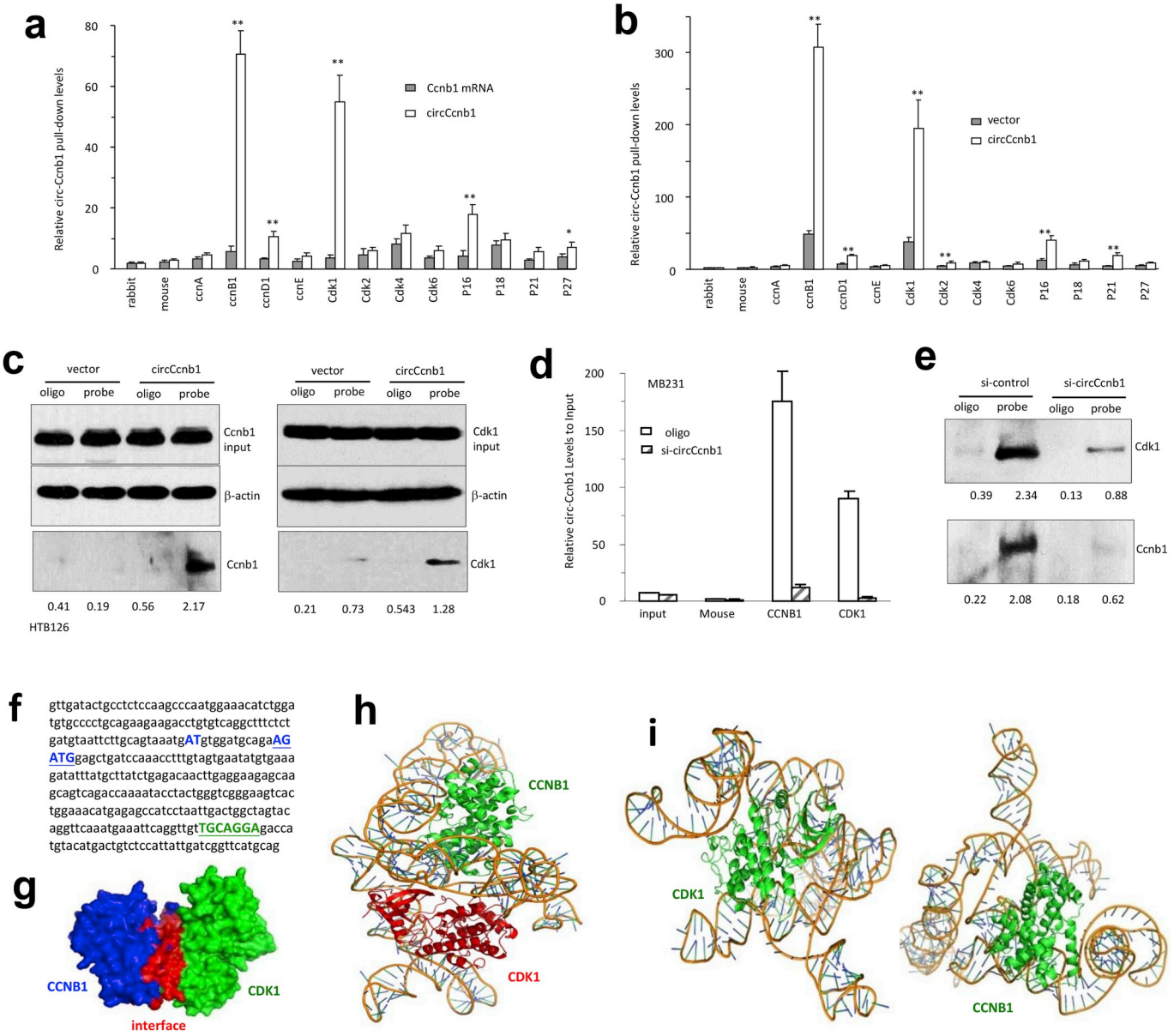

Fig. 1. circ-Ccnb1 binds Ccnb1 and Cdk1. (a) Cell lysate prepared from HTB-126 cells were incubated with antibodies against rabbit IgG, mouse IgG, cyclin A (Ccna), Ccnb1, Ccnd1, Ccne, Cdk1, Cdk2, Cdk4, Cdk6, p16, p18, p21, and p27. The precipitated products were subjected to real-time PCR with primers amplifying circ-Ccnb1 and Ccnb1 mRNA. Antibodies against Ccnb1 and Cdk1 precipitated significantly high amounts of circ-Ccnb1 but not Ccnb1 mRNA. Error bars, SD ($n = 3$). **p < 0.01. (b) Lysates were prepared from HTB-126 cells transfected with circ-Ccnb1 or the vector and incubated with antibodies as above followed by precipitation and real-time PCR. Antibodies against Ccnb1 and Cdk1 precipitated significantly higher levels of circ-Ccnb1 in cells transfected with circ-Ccnb1 than those transfected with the vector. Error bars, SD ($n = 3$). **p < 0.01. (c) The lysates were also incubated with the circ-Ccnb1 probe or a control oligo. The probe pulled down Ccnb1 and Cdk1 in the circ-Ccnb1-transfected cells. (d) Lysates prepared from control oligo- and circ-Ccnb1 siRNA-transfected MB231 cells were incubated with antibodies against rabbit IgG, mouse IgG, Ccnb1 and Cdk1. Silencing endogenous circ-Ccnb1 decreased antibody precipitating circ-Ccnb1. Error bars, SD ($n = 4$). **p < 0.01. (e) The lysates were also incubated with circ-Ccnb1 probe or the control oligo to pull down Ccnb1 and Cdk1 proteins followed by Western blotting. (f) Circ-Ccnb1 showing the key nucleotides that bind to Ccnb1 and Cdk1. (g) Diagram showing the interaction of Ccnb1 and Cdk1. (h) Diagram showing the interaction of circ-Ccnb1 with Cdk1 and Ccnb1. (i) Diagrams showing the interaction of circ-ccnb1 with Cdk1 (left) and Ccnb1 (right).

blocking oligos on cell migration, HTB126 cells were transfected with circ-Ccnb1, vector, oligo blocking Ccnb1 binding site, oligo blocking Cdk1 binding site or both. We found that transfection with circ-Ccnb1 inhibited cell migration, while transfection with either oligo produced similar results. However, transfection with both oligos reversed the effect of circ-Ccnb1 on cell migration (Fig. 5D and E).

In cell invasion assay, HTB126 cells were transfected with circ-Ccnb1 or the control vector. We observed that transfection with circ-Ccnb1 inhibited cell invasion (Fig. 5F). Transfection with circ-Ccnb1 in B16 cells also inhibited cell invasion (Fig. 5G). Silencing circ-Ccnb1 in MDA-MB-231 cells with siRNA targeting circ-Ccnb1 or a control oligo increased cell invasion (Fig. 5H). We then delivered the blocking oligos into HTB126 cells and found that transfection with circ-Ccnb1 inhibited cell invasion. Transfection with either blocking oligo produced similar results. However, transfection with both blocking oligos reversed the effect of circ-Ccnb1 on cell invasion (Fig. 5I). These results suggested that when both blocking oligos were present, circ-Ccnb1 could no longer bind to Ccnb1 and Cdk1. This action freed both proteins allowing them to form Ccnb1-Cdk1 complex and played an opposite effect.

In cell proliferation assay, we transfected HTB126 cells with circ-Ccnb1, vector, oligo blocking Ccnb1 binding site, oligo blocking Cdk1

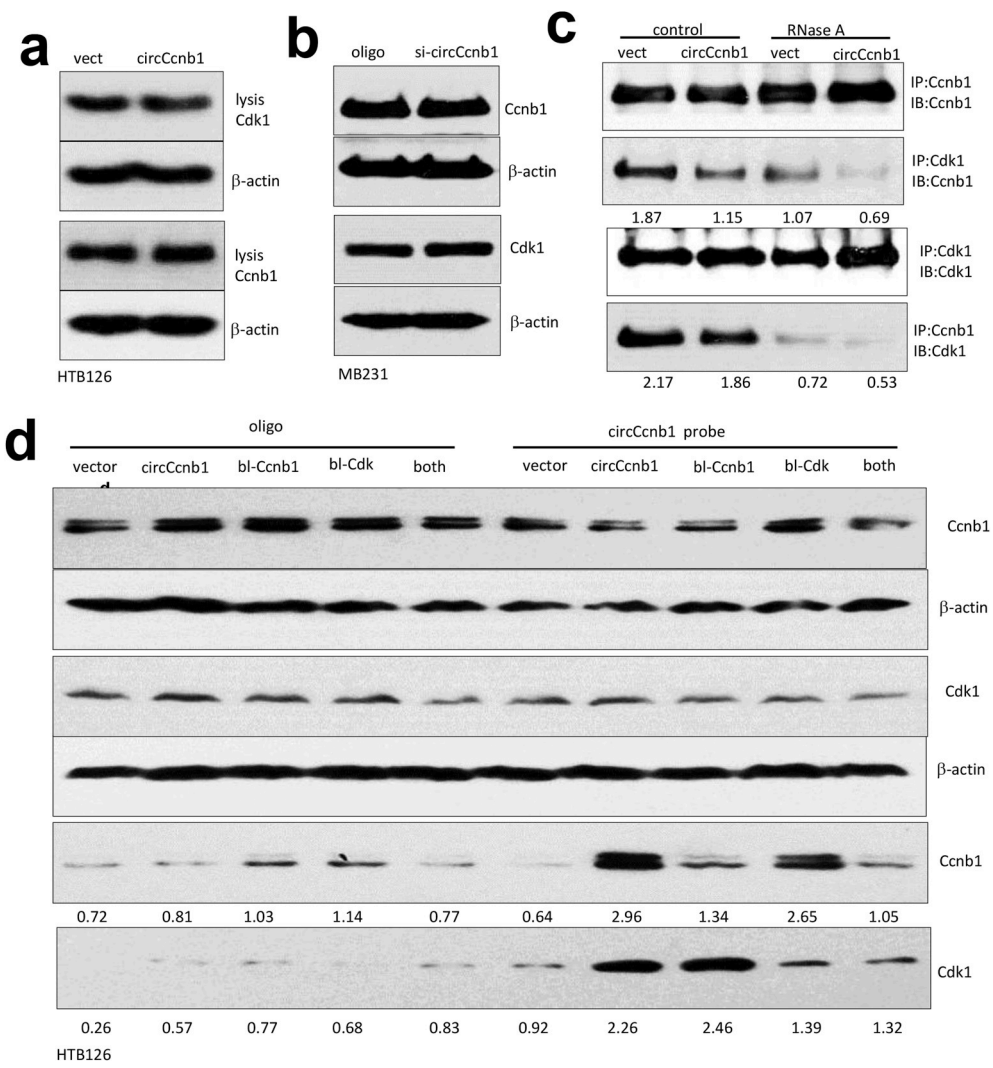

Fig. 2. circ-Ccnb1 forms a ternary complex with Ccnb1 and Cdk1. (a) Lysates prepared from vector- or circ-Ccnb1-transfected HTB126 cells were subject to Western blotting. Expression of Cdk1 and Ccnb1 was not affected by transfection with circ-Ccnb1. (b) Lysates prepared from oligo- or si-ci-Ccnb1-transfected HTB126 cells were subject to Western blotting. Expression of Cdk1 and Ccnb1 was not affected by transfection with siRNA targeting circ-Ccnb1. (c) Lysates prepared from vector- or circ-Ccnb1-transfected HTB126 cells were incubated with RNAse A followed by co-IP and Western blotting. In the presence of RNAse A, Anti-Ccnb1 antibody could no longer precipitate Cdk1 and vice versa. (d) HTB126 cells were transfected with circ-Ccnb1, vector, bl-Cdk (blocking oligo for Cdk1 binding site), bl-Ccn (blocking oligo for Ccnb1 binding site), and both (both blocking oligos). Lysates were prepared and subject to circ-Ccnb1 pull down assay. Transfection with the blocking oligos decreased protein pull down.

binding site or the mixture of both blocking oligos. We found that transfection with circ-Ccnb1 inhibited cell proliferation. Transfection with either oligo produced similar results, but transfection with the mixture of both blocking oligos reversed the effect of circ-Ccnb1 on cell proliferation (Fig. 6A). In cell survival assay, we transfected MDA-MB-231 and B16 cells with circ-Ccnb1 and the control vector and found that expression of circ-Ccnb1 inhibited cell survival (Fig. 6B). HTB126 cells were also transfected with circ-Ccnb1, vector, oligo blocking Ccnb1 binding site, oligo blocking Cdk1 binding site or the mixture of both blocking oligos. While transfection with circ-Ccnb1 inhibited cell survival, and transfection with either oligo produced similar results; transfection with the mix of both blocking oligos reversed the effect of circ-Ccnb1 on cell viability (Fig. 6C). We examined the effects of circ-Ccnb1 transfection on expression of other genes. HTB126 cells transfected with circ-Ccnb1 and the vector displayed increased expression of IL-2, JUNB, and HIF1α, but decreased expression of CDC25A relative to vector control (Fig. 6D).

3.4. Circ-ccnb1 inhibited tumorigenesis and increased mouse survival

We further tested the role of circ-Ccnb1 in mouse tumorigenesis. Regular mice were intraperitoneally injected with B16 cells that were stably transfected with circ-Ccnb1 or the vector. Thirty-five days after cell injection, Kaplan-Meier survival curves was obtained. Mice injected with B16 cells transfected with circ-Ccnb1 significantly survived longer than mice injected with the vector-transfected cells (Fig. 7A). Examination of tumors in the mice revealed that there appeared more tumors with larger sizes in the mice injected with the vector-transfected cells compared with the circ-Ccnb1-trabsfected cells (Fig. 7B). Tumor cells were isolated from the tumor tissues, followed by preparation of total lysate and nuclear fraction. Western blot analysis indicated that the tumors formed by the cells transfected with circ-Ccnb1 or the vector displayed equal amounts of Ccnb1 and Cdk1 (Fig. 7C). However, in the nuclear fractions, the levels of Ccnb1 and Cdk1 were much lower in the circ-Ccnb1 group relative to the vector group (Fig. 7C). The tumor sections were subjected to immunofluorescent staining using antibodies against Ccnb1 and Cdk1. We confirmed that in the tumors formed by cells stably expressing circ-Ccnb1, the levels of Ccnb1 and Cdk1 were higher in cytoplasm but lower in the nuclei relative to tumors formed by the cells transfected with the control vector (Fig. 7D).

Mice were also intraperitoneally injected with B16 cells followed by injection with a control oligo, oligo blocking Ccnb1 binding site, oligo blocking Cdk1 binding site or the mix of both blocking oligos. Forty-three days after the injection, Kaplan-Meier survival curves was obtained. It revealed that injection with the mix of both blocking oligos decreased mouse survival relative to mice injected with the control oligo, the oligo blocking either Ccnb1 or Cdk1 binding site (Fig. 7E). As above, tumor cells were isolated from the tumor tissues. Tumor lysates and nuclear fraction were prepared followed by western blotting. It revealed that transfection with either blocking oligo did not affect expression of Ccnb1 and Cdk1. However, in the nuclear fractions, transfection with the mix of both blocking oligos increased nuclear levels of

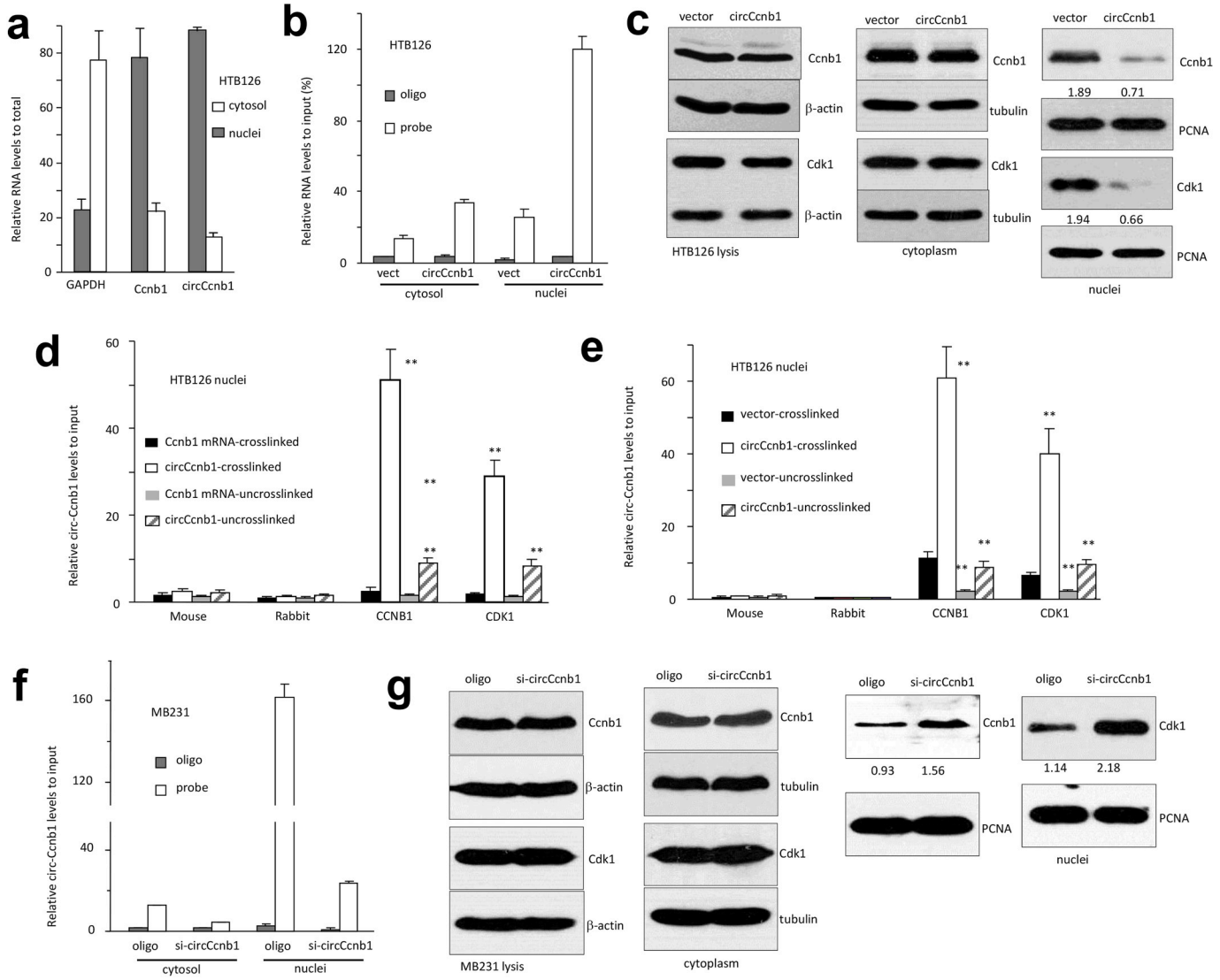

Fig. 3. circ-Ccnb1 inhibits nuclear translocation of Ccnb1 and Cdk1. (a) Cytoplasmic and nuclear fractions were prepared in HTB126 cells for real-time PCR. Circ-Ccnb1 was mainly detected in the nuclei. Error bars, SD ($n = 4$). **p < 0.01. (b) In a pull-down assay, the circ-Ccnb1 probe could pull down significantly higher levels of circ-Ccnb1 than the control oligo. Error bars, SD ($n = 4$). **p < 0.01. (c) Lysate prepared from circ-Ccnb1-and vector-transfected HTB126 cells were subjected to Western blotting. Ectopic expression of circ-Ccnb1 decreased nuclear translocation of Ccnb1 and Cdk1. (d) In immunoprecipitation assay, antibodies against Ccnb1 and Cdk1 precipitated circ-Ccnb1 but not linear Ccnb1 mRNA. The differences were significantly exaggerated by cross-linking treatment. Error bars, SD ($n = 3$). **p < 0.01. (e) In the lysate prepared from the circ-Ccnb1 and vector-transfected HTB126 cells, antibodies against Ccnb1 and Cdk1 precipitated significantly higher levels of circ-Ccnb1 in the circ-Ccnb1-transfected cells than in the vector-transfected cells. Error bars, SD ($n = 3$). **p < 0.01. (f) MDA-MB-231 cells were transfected with siRNA targeting circ-Ccnb1 (si-ci-Cc) or a control oligo. This decreased levels of circ-Ccnb1 pulled down by the circ-Ccnb1 probe in the nuclear fraction. Error bars, SD ($n = 4$). **p < 0.01. (g) In Western blotting, silencing circ-Ccnb1 increased nuclear translocation of Ccnb1 and Cdk1.

Ccnb1 and Cdk1 (Fig. 7F).

4. Discussion

In this study, we found that the circular RNA circ-Ccnb1 could bind to both cyclin B1 (Ccnb1) and Cyclin-dependent kinase 1 (Cdk1) dissociating the formation of cyclin B1-Cdk1 complex. Formation of the ternary complex abolished the roles of Ccnb1 in enhancing cell migration, invasion, proliferation and survival, resulting in inhibition of tumor growth and extension of mouse viability.

Ccnb1 and Cdk1 are highly expressed in breast cancer. These two molecules are key regulatory proteins involved in mitosis. By binding to Cdk1, Ccnb1 functions as an all-or-none switch for commitment to mitosis. It has been reported that both Ccnb1 and Cdk1 are highly expressed in cancer tissues but are not detectable in normal tissues [35–37]. They form cyclin B1-Cdk1 complex which enters the nucleus that is essential for regulation of gene expression and induction of cell mitosis [38,39]. The cyclin B1-Cdk1 complex can also break down the nuclear envelope that is a membrane component containing large protein complexes. This complex is integrated into the lamin network. The cyclin B1-Cdk1 complex can phosphorylate lamins leading to dissociation of the net work, which is essential as it facilitates the access of mitotic spindle to chromosomes [40]. Our results showed that the circular RNA circ-Ccnb1 binds to both Ccnb1 and Cdk1, inhibiting the formation of the cyclin B1-Cdk1 complex and their entry into nucleus. Thus, Ccnb1 and Cdk1 can no longer exert their mitotic activity.

Before forming a complex with Cdk1 and entering the nucleus, cyclin B1 is located in cytoplasm, where it is inactive. Activation of the complex is achieved by dephosphorylation by Cdc25 phosphatase [41]. Prior to its relocation to the nucleus, cyclin B1 must be phosphorylated, a key step for cyclin B1-Cdk1 complex imported to nucleus [42]. Cyclin B1 is phosphorylated by Cdk1 and Polo kinase. Cyclin B1

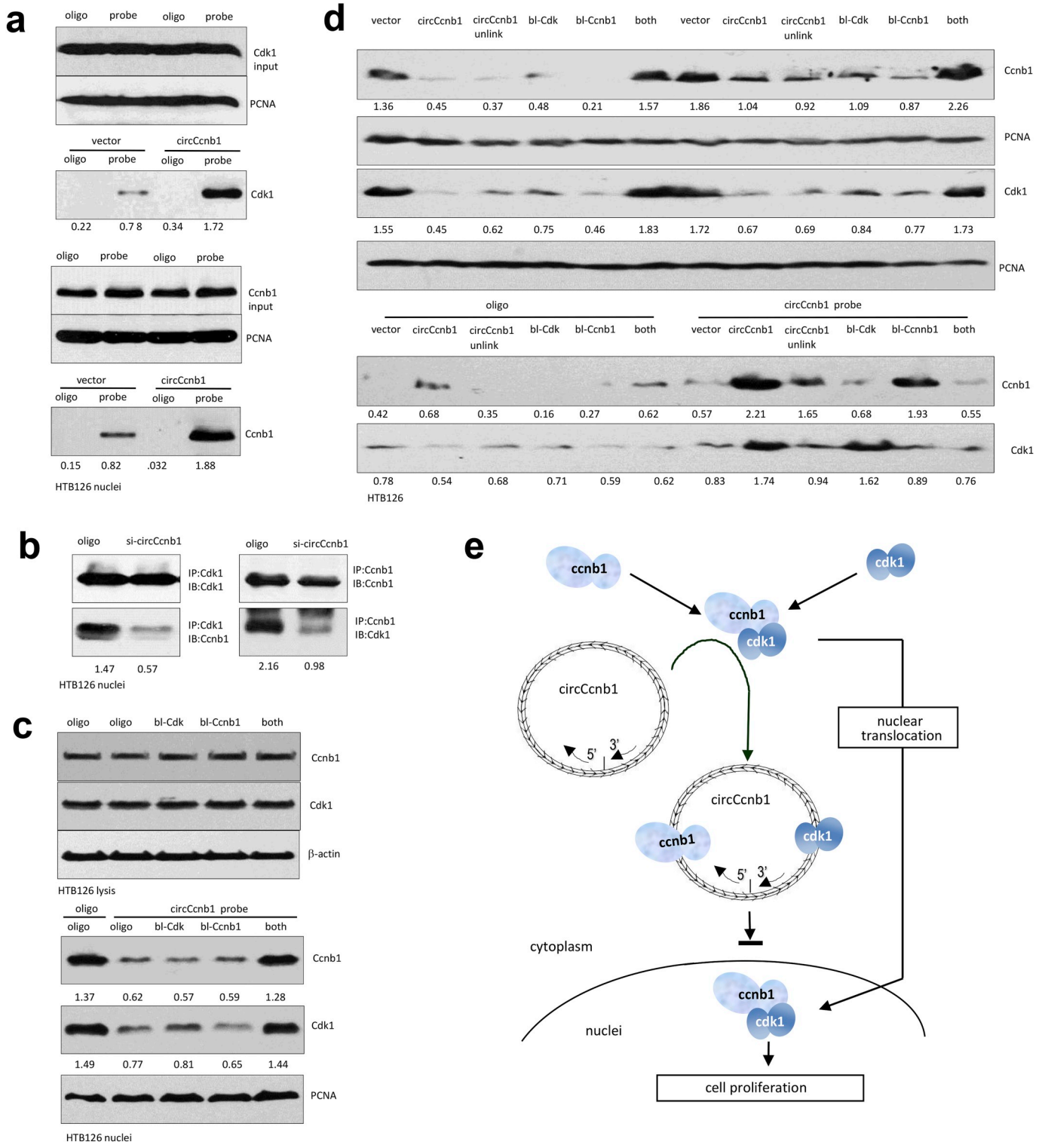

Fig. 4. The interaction of circ-Ccnb1 is essential for nuclear translocation of Ccnb1 and Cdk1. (a) Nuclear fractions were prepared from the circ-Ccnb1-and vector-transfected HTB126 cells, followed by incubation with circ-Ccna1 probe or a control oligo. The pull-down mixture was subjected to western blotting probed by antibodies against Cdk1 or Ccnb1. (b) Antibody against Cdk1 precipitated lower levels of Ccnb1 in the cells transfected with circ-Ccnb1 siRNA than the cells transfected with the control oligo, and vice versa. (c) Upper, Transfection with the blocking oligos did not affect expression of Ccnb1 and Cdk1. Lower, Transfection with either oligo blocking Ccnb1 binding site or oligo blocking Cdk1 binding site did not affect nuclear translocation of Ccnb1 and Cdk1. Transfection with both blocking oligos increased levels of Ccnb1 and Cdk1 in the nuclei. (d) HTB126 cells were transfected with vector, circ-Ccnb1, circ-Ccnb1 (without cross-liking), bl-Cdk (blocking oligo for Cdk1 binding site), bl-Ccn (blocking oligo for Ccnb1 binding site), and both (both blocking oligos), followed by cross-linking. Lysates were prepared and subject to circ-Ccnb1 pull down assay. Transfection with the blocking oligos decreased protein pull down. (e) A diagram showing the effect of circ-Ccnb1 on regulating functions of Ccnb1 and Cdk1.

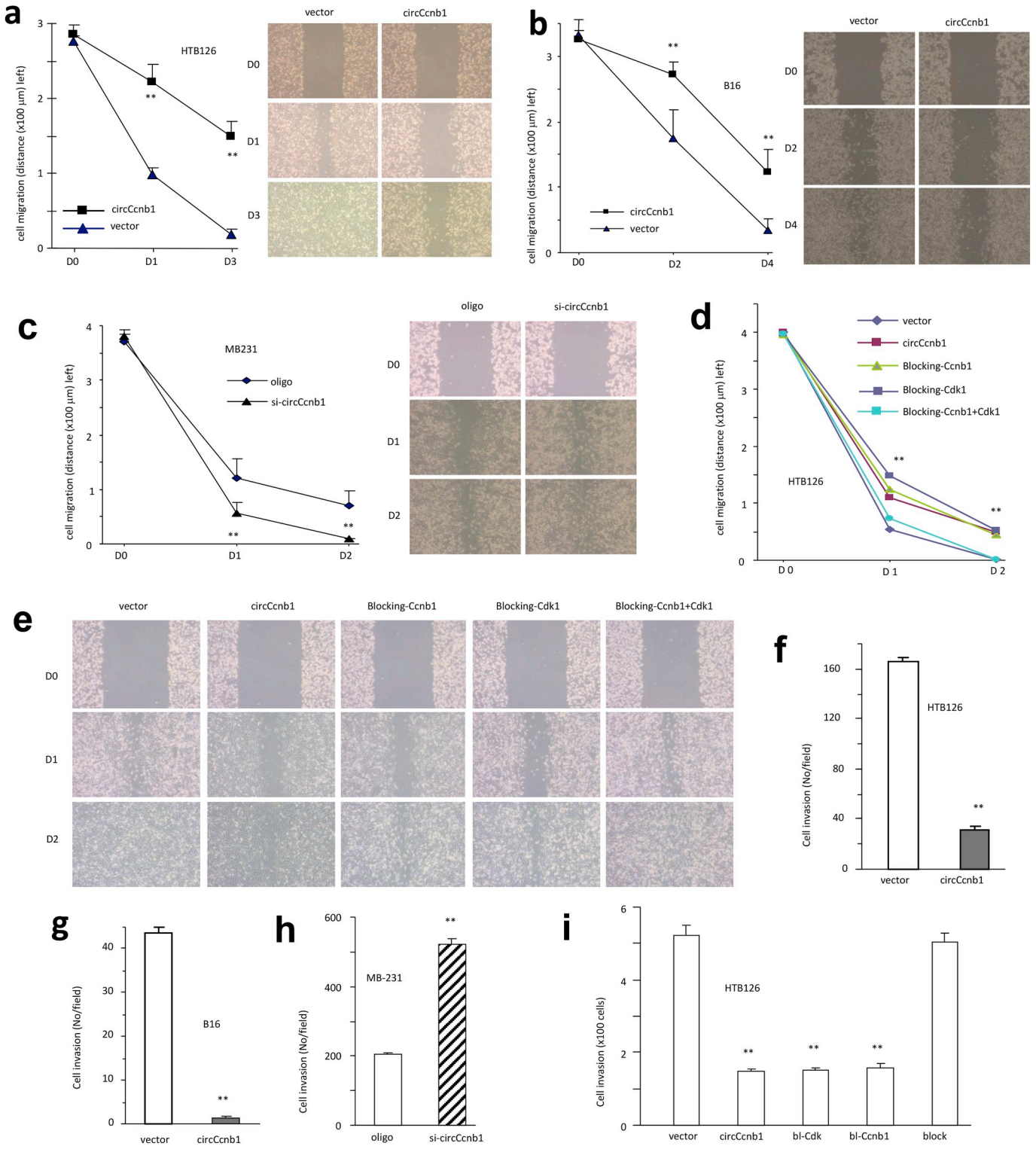

Fig. 5. circ-Ccnb1 inhibited breast cancer cell migration and invasion.(a–b) The migration was determined in HTB126 (a) and B16 (b) cells stably transfected with circ-Ccn1 or the vector. Overexpression of circ-Ccnb1 inhibited cell migration. Error bars, SD ($n = 4$). **p < 0.01 (left). Typical cell photos are shown (right). (c) MDA-MB-231 cells were transfected with siRNA targeting circ-Ccnb1 or a control oligo. Silencing circ-Ccnb1 increased cell migration. Error bars, SD ($n = 4$). **p < 0.01 (left). Typical cell photos are shown (right). (d–e) HTB126 cells were transfected with circ-Ccnb1, vector, oligo blocking Ccnb1 binding site, oligo blocking Cdk1 binding site or both. Transfection with circ-Ccnb1 inhibited cell migration. Transfection with either oligo produced similar results. Transfection with both oligos reversed the effect of circ-Ccnb1 on cell migration. Error bars, SD ($n = 4$). **p < 0.01 (d). Typical cell photos are shown (e). (f) HTB126 cells were transfected with circ-Ccnb1 or vector, followed by cell invasion assay. Transfection with circ-Ccnb1 inhibited cell invasion. Error bars, SD ($n = 4$). **p < 0.01. (g) Transfection with circ-Ccnb1 inhibited B16 cell invasion. Error bars, SD ($n = 4$). **p < 0.01. (h) MDA-MB-231 cells were transfected with siRNA targeting circ-Ccnb1 or a control oligo. Silencing circ-Ccnb1 increased cell invasion. Error bars, SD ($n = 4$). **p < 0.01. (i) HTB126 cells were transfected with circ-Ccnb1, vector, oligo blocking Ccnb1 binding site, oligo blocking Cdk1 binding site or both. Transfection with circ-Ccnb1 inhibited cell invasion. Transfection with either oligo produced similar results. Transfection with both oligos reversed the effect of circ-Ccnb1 on cell invasion. Error bars, SD ($n = 4$). **p < 0.01.

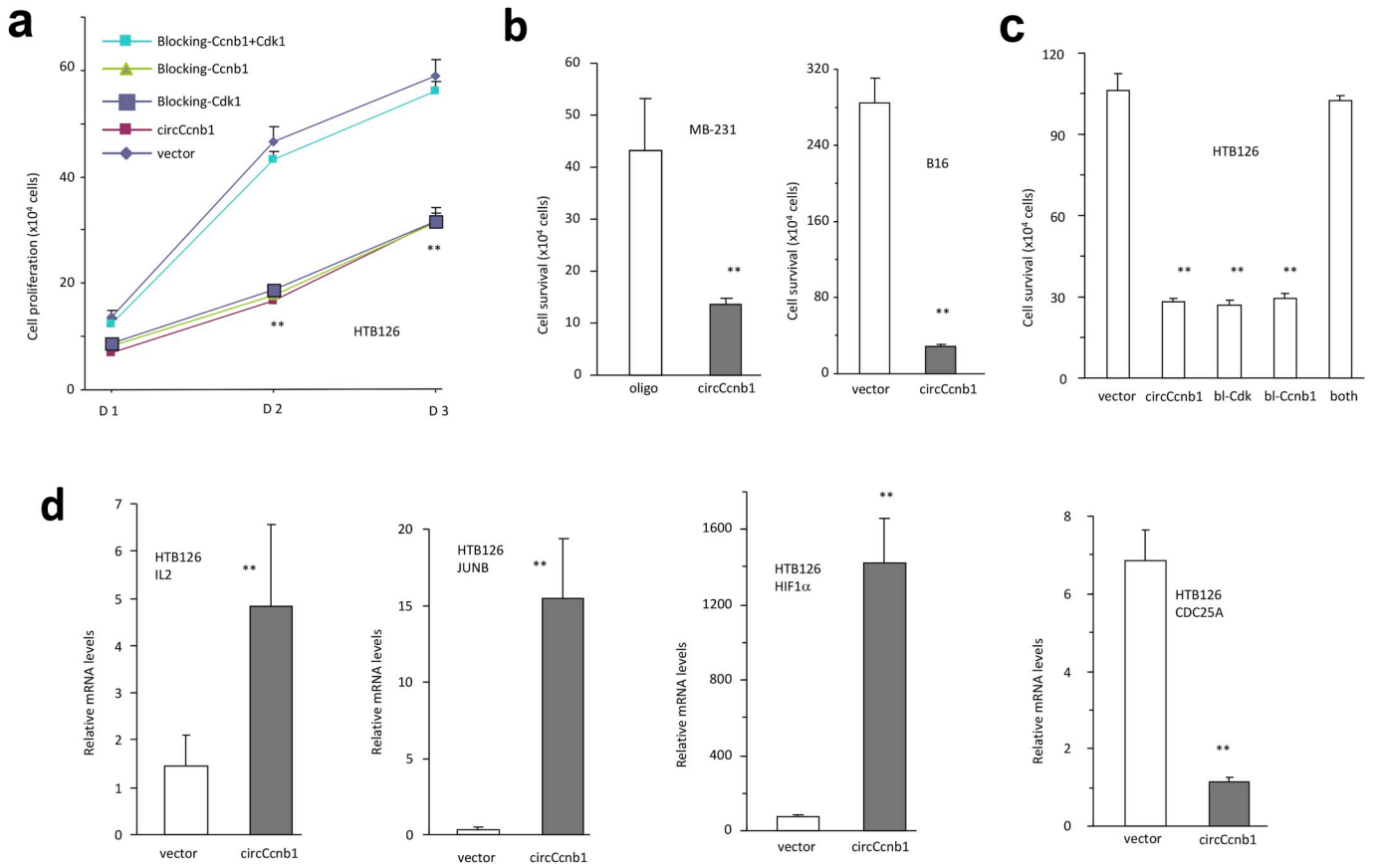

Fig. 6. circ-Ccnb1 inhibited breast cancer cell proliferation and survival. (a) HTB126 cells were transfected with circ-Ccnb1, vector, oligo blocking Ccnb1 binding site, oligo blocking Cdk1 binding site or both. Transfection with circ-Ccnb1 inhibited cell proliferation. Transfection with either oligo produced similar results. Transfection with both oligos reversed the effect of circ-Ccnb1 on cell proliferation. Error bars, SD ($n = 4$). **p < 0.01. (b) MDA-MB-23 (left) and B16 (right) cells were transfected with circ-Ccnb1 followed by cell viability assay. Expression of circ-Ccnb1 inhibited cell viability. Error bars, SD ($n = 4$). **p < 0.01. (c) HTB126 cells were transfected with circ-Ccnb1, vector, oligo blocking Ccnb1 binding site, oligo blocking Cdk1 binding site or both. Transfection with circ-Ccnb1 inhibited cell survival. Transfection with either oligo produced similar results. Transfection with both oligos reversed the effect of circ-Ccnb1 on cell viability. Error bars, SD ($n = 4$). **p < 0.01. (d) HTB126 cells were transfected with circ-Ccnb1 and vector followed by gene expression determination. Transfection with circ-Ccnb1 increased expression of IL-2, JUNB, and HIF1α, but decreased expression of CDC25A relative to vector control.

Phosphorylation prevents its export from the nucleus [43]. The activated cyclin B1-Cdk1 complex remains stable for the rest of the mitotic cycle. It is not clear whether interaction of circ-Ccnb1 with Ccnb1 and Cdk1 can prevent activation of these two molecules and decrease cell cycle progression.

The cyclin B1-Cdk1 complex plays important roles in the transition of the cell from G2 to M phase. In tumor cells, cyclin B1 is over expressed and its overexpression is loss of control. The unregulated cyclin B1 binds to its partner Cdks and promote cancer cell growth. Although the exact mechanism by which cyclin B1 becomes overexpressed is not well understood, it is known that cyclin B1 is essential for tumor cell survival and proliferation. Decreased expression of cyclin B1 causes tumor cell death specifically [44]. It can stop cells in the G2 phase and trigger cell death by preventing the chromosome condensation. Downregulation of cyclin B1 has no effect on the expression and activities of other molecules involving in the transition from the G2 to M phase. Thus, targeting cyclin B1 can serve as a therapeutic approach for tumor suppression [45]. A possible approach is to deliver gene or protein to induce degradation of cyclin B1. Alternatively, drugs are developed targeting these mitotic molecules [46,47].

Novel mechanisms that mitigate the aberrant mitotic activities induced by the cyclin B1-Cdk1 complex is key to produce new intervention in cancer progression. Since circ-Ccnb1 can prevent the interaction between Ccnb1 and Cdk1, the cyclin B1-Cdk1 complex cannot be formed. Our results showed that ectopic delivery of circ-Ccnb1 could be up-taken by the tumor cells, and the exogenous circ-Ccnb1 displayed the same activity in binding to Ccnb1 and Cdk1. The binding sites of circ-Ccnb1 to these two proteins are sufficiently distal to one another, resulting in the dissociation of Ccnb1 from Cdk1. It should be noted that circ-Ccnb1 could not only bind Ccnb1 and Cdk1 in cytoplasm, but also in nucleus. These results suggest that circ-Ccnb1 is a powerful circular RNA in the inhibition of tumor progression. Circular RNAs have recently been reported to play roles in cancer development [18,48–50]. Our recent publication showed that circ-Ccnb1 binds to H2AX and inhibits mutant p53 binding leading cancer cell apoptosis [32]. Our results here showed that circ-Ccnb1 could also bind to Ccnb1 and Cdk1, inhibiting the formation of cyclin B1-Cdk1 complex and inducing cancer cell death. It thus adds another mechanism for circ-Ccnb1 to suppress cancer progression. The development of technology to safely delivery circ-Ccnb1 clinically for patient treatment will be a promising task in the future. Nanotechnology appears to be effective in delivering circ-Ccnb1 into tumor-bearing mice. However, the safety of nanotechnology in human awaits further investigation.Acknowledgements

This work was supported by grants from Canadian Institutes of Health Research (PJT-153105 and PJT-155962), the National Natural Science Foundation of China (81602334), the Natural Science Foundation of Guangdong Province (2016A030310285), Guangzhou Science and Technology Plan Project (201604016051), and Innovation and Entrepreneurship Leading Talent of Guangzhou Development Zone (2017-L181).

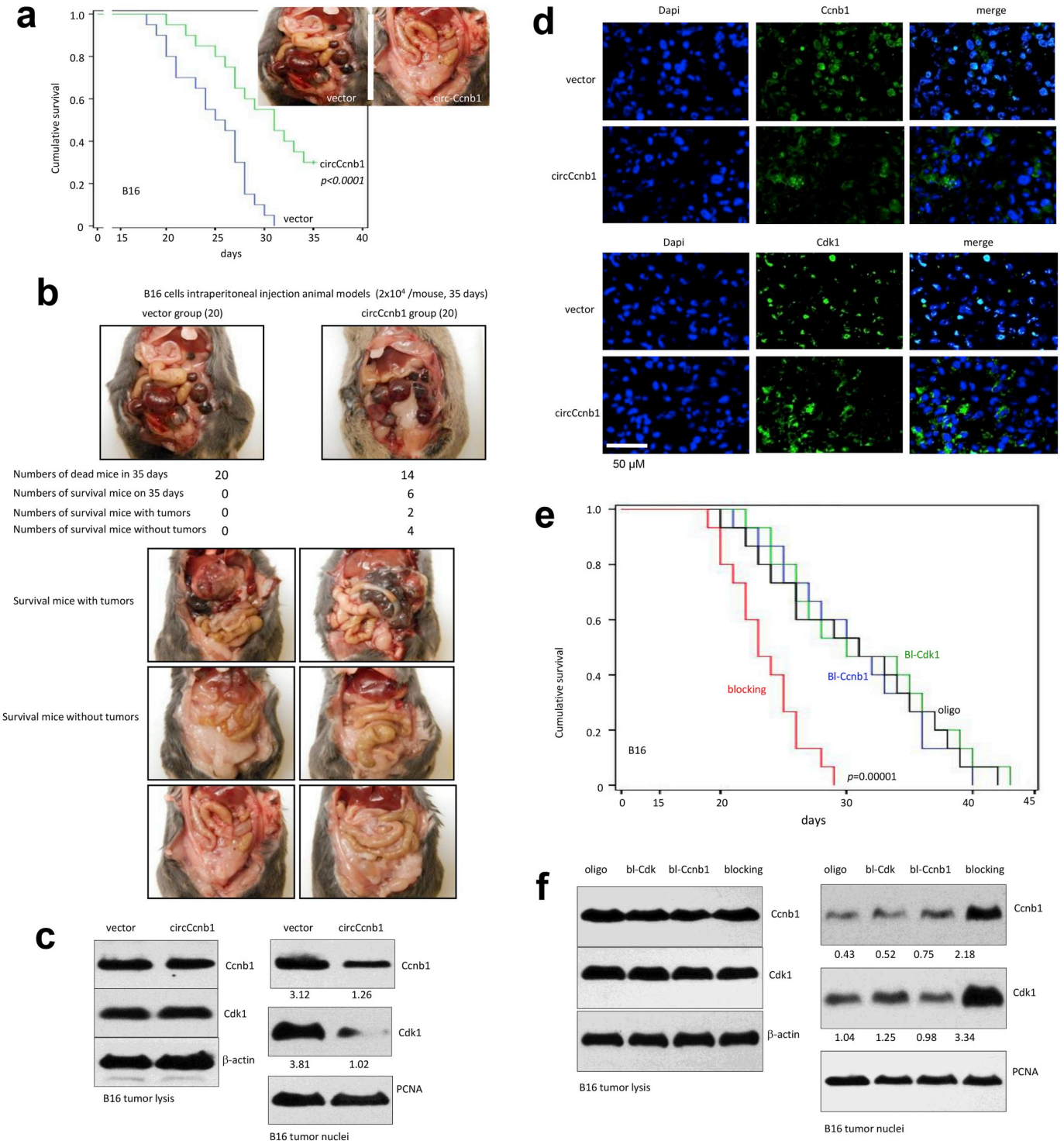

Fig. 7. Circ-Ccnb1 inhibited tumorigenesis. (a) Mice were intraperitoneally injected with B16 cells stably transfected with circ-Ccnb1 or the vector. Kaplan-Meier survival curves was obtained. Mice injected with B16 cells transfected with circ-Ccnb1 survived significantly longer than mice injected with the vector-transfected cells. n = 20, p < 0.0001. (b) Some mice with typical tumor formation are shown. (c) Tumor cells were isolated from the tumor tissues. Tumor lysates and nuclear fraction were prepared followed by western blotting. Both tumors formed by the cells transfected with circ-Ccnb1 or the vector displayed equal amounts of Ccnb1 and Cdk1. In the nuclear fractions, expression of circ-Ccnb1 decreased nuclear levels of Ccnb1 and Cdk1. (d) The tumor sections were subjected to immunofluorescent staining. Expression of circ-Ccnb1 decreased nuclear localization of Ccnb1 and Cdk1. (e) Mice were intraperitoneally injected with B16 cells followed by injection with a control oligo, oligo blocking Ccnb1 binding site, oligo blocking Cdk1 binding site or both. Kaplan-Meier survival curves was obtained. Injection with both oligos decreased mouse survival relative to mice injected with the control oligo, the oligo blocking either Ccnb1 or Cdk1 binding site. n = 20, **, p < 0.00001. (f) Tumor lysates and nuclear fraction were prepared followed by western blotting. Transfection with the blocking oligos did not affect expression of Ccnb1 and Cdk1. In the nuclear fractions, transfection with both oligos increased nuclear levels of Ccnb1 and Cdk1.

Conflicts of interest

The authors declare no conflict of interest.

References

[1] Y. Enuka, M. Lauriola, M.E. Feldman, A. Sas-Chen, I. Ulitsky, Y. Yarden, Circular RNAs are long-lived and display only minimal early alterations in response to a growth factor, Nucleic Acids Res. 44 (2016) 1370–1383.

[2] W.R. Jeck, N.E. Sharpless, Detecting and characterizing circular RNAs, Nat. Biotechnol. 32 (2014) 453–461.

[3] Y.C. Liu, J.R. Li, C.H. Sun, E. Andrews, R.F. Chao, F.M. Lin, S.L. Weng, S.D. Hsu, C.C. Huang, C. Cheng, C.C. Liu, H.D. Huang, CircNet: a database of circular RNAs derived from transcriptome sequencing data, Nucleic Acids Res. 44 (2016) D209–D215.

[4] W.R. Jeck, J.A. Sorrentino, K. Wang, M.K. Slevin, C.E. Burd, J. Liu, W.F. Marzluff, N.E. Sharpless, Circular RNAs are abundant, conserved, and associated with ALU repeats, Rna 19 (2013) 141–157.

[5] S. Memczak, M. Jens, A. Elefsinioti, F. Torti, J. Krueger, A. Rybak, L. Maier, S.D. Mackowiak, L.H. Gregersen, M. Munschauer, A. Loewer, U. Ziebold, M. Landthaler, C. Kocks, F. le Noble, N. Rajewsky, Circular RNAs are a large class of animal RNAs with regulatory potency, Nature 495 (2013) 333–338.

[6] L.L. Zheng, J.H. Li, J. Wu, W.J. Sun, S. Liu, Z.L. Wang, H. Zhou, J.H. Yang, L.H. Qu, deepBase v2.0: identification, expression, evolution and function of small RNAs, LncRNAs and circular RNAs from deep-sequencing data, Nucleic Acids Res. 44 (2016) D196–D202.

[7] Y. Zhang, X.O. Zhang, T. Chen, J.F. Xiang, Q.F. Yin, Y.H. Xing, S. Zhu, L. Yang, L.L. Chen, Circular intronic long noncoding RNAs, Mol. Cell 51 (2013) 792–806.

[8] Z. Li, C. Huang, C. Bao, L. Chen, M. Lin, X. Wang, G. Zhong, B. Yu, W. Hu, L. Dai, P. Zhu, Z. Chang, Q. Wu, Y. Zhao, Y. Jia, P. Xu, H. Liu, G. Shan, Exon-intron circular RNAs regulate transcription in the nucleus, Nat. Struct. Mol. Biol. 22 (2015) 256–264.

[9] T.B. Hansen, T.I. Jensen, B.H. Clausen, J.B. Bramsen, B. Finsen, C.K. Damgaard, J. Kjems, Natural RNA circles function as efficient microRNA sponges, Nature 495 (2013) 384–388.

[10] Y. Bai, Y. Zhang, B. Han, L. Yang, X. Chen, R. Huang, F. Wu, J. Chao, P. Liu, G. Hu, J.H. Zhang, H. Yao, Circular RNA DLGAP4 ameliorates ischemic stroke outcomes by targeting miR-143 to regulate endothelial-mesenchymal transition associated with blood-brain barrier integrity, J. Neurosci. : the official journal of the Society for Neuroscience 38 (1) (2018 Jan 3) 32–50, https://doi.org/10.1523/JNEUROSCI.1348-17.2017 Epub 2017 Nov 7.

[11] R. Huang, Y. Zhang, B. Han, Y. Bai, R. Zhou, G. Gan, J. Chao, G. Hu, H. Yao, Circular RNA HIPK2 regulates astrocyte activation via cooperation of autophagy and ER stress by targeting MIR124-2HG, Autophagy 13 (2017) 1722–1741.

[12] W. Yang, W.W. Du, X. Li, A.J. Yee, B.B. Yang, Foxo3 activity promoted by non-coding effects of circular RNA and Foxo3 pseudogene in the inhibition of tumor growth and angiogenesis, Oncogene 35 (2016) 3919–3931.

[13] B. Capel, A. Swain, S. Nicolis, A. Hacker, M. Walter, P. Koopman, P. Goodfellow, R. Lovell-Badge, Circular transcripts of the testis-determining gene Sry in adult mouse testis, Cell 73 (1993) 1019–1030.

[14] J. Salzman, C. Gawad, P.L. Wang, N. Lacayo, P.O. Brown, Circular RNAs are the predominant transcript isoform from hundreds of human genes in diverse cell types, PLoS One 7 (2012) e30733.

[15] W.W. Du, L. Fang, W. Yang, N. Wu, F.M. Awan, Z. Yang, B.B. Yang, Induction of tumor apoptosis through a circular RNA enhancing Foxo3 activity, Cell Death Differ. 24 (2017) 357–370.

[16] W.W. Du, W. Yang, Y. Chen, Z.K. Wu, F.S. Foster, Z. Yang, X. Li, B.B. Yang, Foxo3 circular RNA promotes cardiac senescence by modulating multiple factors associated with stress and senescence responses, Eur. Heart J. 38 (2017) 1402–1412.

[17] W.W. Du, W. Yang, E. Liu, Z. Yang, P. Dhaliwal, B.B. Yang, Foxo3 circular RNA retards cell cycle progression via forming ternary complexes with p21 and CDK2, Nucleic Acids Res. 44 (2016) 2846–2858.

[18] Y. Chen, F. Yang, E. Fang, W. Xiao, H. Mei, H. Li, D. Li, H. Song, J. Wang, M. Hong, X. Wang, K. Huang, L. Zheng, Q. Tong, Circular RNA circAGO2 drives cancer progression through facilitating HuR-repressed functions of AGO2-miRNA complexes, Cell Death Differ. 26 (7) (2019 Jul) 1346–1364, https://doi.org/10.1038/s41418-018-0220-6 Epub 2018 Oct 19.

[19] N. Wu, Z. Yuan, K.Y. Du, L. Fang, J. Lyu, C. Zhang, A. He, E. Eshaghi, K. Zeng, J. Ma, W.W. Du, B.B. Yang, Translation of yes-associated protein (YAP) was antagonized by its circular RNA via suppressing the assembly of the translation initiation machinery, Cell Death Differ. (2019 May 15), https://doi.org/10.1038/s41418-019-0337-2 [Epub ahead of print].

[20] X. Zhang, Y. Xu, Z. Qian, W. Zheng, Q. Wu, Y. Chen, G. Zhu, Y. Liu, Z. Bian, W. Xu, Y. Zhang, F. Sun, Q. Pan, J. Wang, L. Du, Y. Yu, circRNA_104075 stimulates YAP-dependent tumorigenesis through the regulation of HNF4a and may serve as a diagnostic marker in hepatocellular carcinoma, Cell Death Dis. 9 (2018) 1091.

[21] J. Yuan, A. Kramer, Y. Matthess, R. Yan, B. Spankuch, R. Gatje, R. Knecht, M. Kaufmann, K. Strebhardt, Stable gene silencing of cyclin B1 in tumor cells increases susceptibility to taxol and leads to growth arrest in vivo, Oncogene 25 (2006) 1753–1762.

[22] R.D. Mashal, S. Lester, C. Corless, J.P. Richie, R. Chandra, K.J. Propert, A. Dutta, Expression of cell cycle-regulated proteins in prostate cancer, Cancer Res. 56 (1996) 4159–4163.

[23] Q. Zhan, M.J. Antinore, X.W. Wang, F. Carrier, M.L. Smith, C.C. Harris, A.J. Fornace Jr., Association with Cdc2 and inhibition of Cdc2/Cyclin B1 kinase activity by the p53-regulated protein Gadd45, Oncogene 18 (1999) 2892–2900.

[24] S. Jin, M.J. Antinore, F.D. Lung, X. Dong, H. Zhao, F. Fan, A.B. Colchagie, P. Blanck, P.P. Roller, A.J. Fornace Jr., Q. Zhan, The GADD45 inhibition of Cdc2 kinase correlates with GADD45-mediated growth suppression, J. Biol. Chem. 275 (2000) 16602–16608.

[25] G.M. Kupfer, T. Yamashita, D. Naf, A. Suliman, S. Asano, A.D. D'Andrea, The Fanconi anemia polypeptide, FAC, binds to the cyclin-dependent kinase, cdc2, Blood 90 (1997) 1047–1054.

[26] Q. Yang, A. Manicone, J.D. Coursen, S.P. Linke, M. Nagashima, M. Forgues, X.W. Wang, Identification of a functional domain in a GADD45-mediated G2/M checkpoint, J. Biol. Chem. 275 (2000) 36892–36898.

[27] X. Yang, W.W. Du, H. Li, F. Liu, A. Khorshidi, Z.J. Rutnam, B.B. Yang, Both mature miR-17-5p and passenger strand miR-17-3p target TIMP3 and induce prostate tumor growth and invasion, Nucleic Acids Res. 41 (2013) 9688–9704.

[28] Z.J. Rutnam, W.W. Du, W. Yang, X. Yang, B.B. Yang, The pseudogene TUSC2P promotes TUSC2 function by binding multiple microRNAs, Nat. Commun. 5 (2014) 2914.

[29] W.W. Du, W. Yang, Y. Chen, Z.K. Wu, F.S. Foster, Z. Yang, X. Li, B.B. Yang, Foxo3 circular RNA promotes cardiac senescence by modulating multiple factors associated with stress and senescence responses, Eur. Heart J. 38 (18) (2017 May 7) 1402–1412, https://doi.org/10.1093/eurheartj/ehw001.

[30] I. Tuszynska, M. Magnus, K. Jonak, W. Dawson, J.M. Bujnicki, NPDock: a web server for protein-nucleic acid docking, Nucleic Acids Res. 43 (2015) W425–W430.

[31] M.J. Pietal, N. Szostak, K.M. Rother, J.M. Bujnicki, RNAmap2D - calculation, visualization and analysis of contact and distance maps for RNA and protein-RNA complex structures, BMC Bioinf. 13 (2012) 333.

[32] L. Fang, W.W. Du, J. Lyu, J. Dong, C. Zhang, W. Yang, A. He, Y.S.S. Kwok, J. Ma, N. Wu, F. Li, F.M. Awan, C. He, B.L. Yang, C. Peng, H.J. MacKay, A.J. Yee, B.B. Yang, Enhanced breast cancer progression by mutant p53 is inhibited by the circular RNA circ-Ccnb1, Cell Death Differ. 25 (12) (2018 Dec) 2195–2208, https://doi.org/10.1038/s41418-018-0115-6 Epub 2018 May 23.

[33] Y. Zeng, W.W. Du, Y. Wu, Z. Yang, F.M. Awan, X. Li, W. Yang, C. Zhang, Q. Yang, A. Yee, Y. Chen, F. Yang, H. Sun, R. Huang, A.J. Yee, R.K. Li, Z. Wu, P.H. Backx, B.B. Yang, A circular RNA binds to and activates AKT phosphorylation and nuclear localization reducing apoptosis and enhancing cardiac repair, Theranostics 7 (2017) 3842–3855.

[34] M. Jackman, C. Lindon, E.A. Nigg, J. Pines, Active cyclin B1-Cdk1 first appears on centrosomes in prophase, Nat. Cell Biol. 5 (2003) 143–148.

[35] Q. Xi, M. Huang, Y. Wang, J. Zhong, R. Liu, G. Xu, L. Jiang, J. Wang, Z. Fang, S. Yang, The expression of CDK1 is associated with proliferation and can be a prognostic factor in epithelial ovarian cancer, Tumour Biol 36 (2015) 4939–4948.

[36] T. Bae, K.Y. Weon, J.W. Lee, K.H. Eum, S. Kim, J.W. Choi, Restoration of paclitaxel resistance by CDK1 intervention in drug-resistant ovarian cancer, Carcinogenesis 36 (2015) 1561–1571.

[37] C.C. Chang, C.M. Hung, Y.R. Yang, M.J. Lee, Y.C. Hsu, Sulforaphane induced cell cycle arrest in the G2/M phase via the blockade of cyclin B1/CDC2 in human ovarian cancer cells, J. Ovarian Res. 6 (2013) 41.

[38] M. Sano, Y. Ichimaru, M. Kurita, E. Hayashi, T. Homma, H. Saito, S. Masuda, N. Nemoto, A. Hemmi, T. Suzuki, S. Miyairi, H. Hao, Induction of cell death in pancreatic ductal adenocarcinoma by indirubin 3'-oxime and 5-methoxyindirubin 3'-oxime in vitro and in vivo, Cancer Lett. 397 (2017) 72–82.

[39] X.Q. Wang, C.M. Lo, L. Chen, E.S. Ngan, A. Xu, R.Y. Poon, CDK1-PDK1-PI3K/Akt signaling pathway regulates embryonic and induced pluripotency, Cell Death Differ. 24 (2017) 38–48.

[40] R. Heald, F. McKeon, Mutations of phosphorylation sites in lamin A that prevent nuclear lamina disassembly in mitosis, Cell 61 (1990) 579–589.

[41] J.M. Enserink, R.D. Kolodner, An overview of Cdk1-controlled targets and processes, Cell Div. 5 (2010) 11.

[42] H.L. De Bondt, J. Rosenblatt, J. Jancarik, H.D. Jones, D.O. Morgan, S.H. Kim, Crystal structure of cyclin-dependent kinase 2, Nature 363 (1993) 595–602.

[43] P.D. Jeffrey, A.A. Russo, K. Polyak, E. Gibbs, J. Hurwitz, J. Massague, N.P. Pavletich, Mechanism of CDK activation revealed by the structure of a cyclinA-CDK2 complex, Nature 376 (1995) 313–320.

[44] M. Vairapandi, A.G. Balliet, B. Hoffman, D.A. Liebermann, GADD45b and GADD45g are cdc2/cyclinB1 kinase inhibitors with a role in S and G2/M cell cycle checkpoints induced by genotoxic stress, J. Cell. Physiol. 192 (2002) 327–338.

[45] J. Pines, T. Hunter, Isolation of a human cyclin cDNA: evidence for cyclin mRNA and protein regulation in the cell cycle and for interaction with p34cdc2, Cell 58 (1989) 833–846.

[46] M. Gao, B. Li, X. Sun, Y. Zhou, Y. Wang, V.S. Tompkins, Z. Xu, N. Indima, H. Wang, W. Xiao, L. Gao, G. Chen, H. Wu, X. Wu, Y. Kong, B. Xie, Y. Zhang, G. Chang, L. Hu, G. Yang, B. Dai, Y. Tao, W. Zhu, J. Shi, Preclinical activity of DCZ3301, a novel arylguanidino compound in the therapy of multiple myeloma, Theranostics 7 (2017) 3690–3699.

[47] L. Porcelli, D. Stolfa, A. Stefanachi, R. Di Fonte, M. Garofoli, R.M. Iacobazzi, N. Silvestris, A. Guarini, S. Cellamare, A. Azzariti, Synthesis and biological evaluation OF N-biphenyl-nicotinic based Moiety compounds: a new class of anti-mitotic agents for the treatment of Hodgkin lymphoma, Cancer Lett. 445 (2019 Mar 31) 1–10, https://doi.org/10.1016/j.canlet.2018.12.013 Epub 2018 Dec 22.

[48] B. Chen, W. Wei, X. Huang, X. Xie, Y. Kong, D. Dai, L. Yang, J. Wang, H. Tang, X. Xie, circEPSTI1 as a prognostic marker and mediator of triple-negative breast cancer progression, Theranostics 8 (2018) 4003–4015.

[49] H. Teng, F. Mao, J. Liang, M. Xue, W. Wei, X. Li, K. Zhang, D. Feng, B. Liu, Z. Sun, Transcriptomic signature associated with carcinogenesis and aggressiveness of papillary thyroid carcinoma, Theranostics 8 (2018) 4345–4358.

[50] Z. Yang, L. Xie, L. Han, X. Qu, Y. Yang, Y. Zhang, Z. He, Y. Wang, J. Li, Circular RNAs: regulators of cancer-related signaling pathways and potential diagnostic biomarkers for human cancers, Theranostics 7 (2017) 3106–3117.